Crystal Structure and Magnetic Properties of an Octacyanometalate-Based Three-Dimensional Tungstate(V)−Manganese(II) Bimetallic Assembly

Zhuang Jin Zhong,[1a] Hidetake Seino,[1b] Yasushi Mizobe,[1b] Masanobu Hidai,[1c] Michel Verdaguer,[1d] Shin-ichi Ohkoshi,[1e] and Kazuhito Hashimoto*[,1a,e]

Kanagawa Academy of Science and Technology, 3-2-1 Sakato, Takatsu-ku, Kawasaki, Kanagawa 213, Japan, Institute of Industrial Science, The University of Tokyo, 7-22-1 Roppongi, Minato-ku, Tokyo 106-8558, Japan, Department of Materials Science and Technology, Science University of Tokyo, Noda, Chiba 278-8510, Japan, Laboratoire de Chimie Inorganique et Matériaux Moléculaires, Unité CNRS 7071, Université Pierre et Marie Curie, 4 Place Jussieu, 75252 Paris Cedex 05, France, and Research Center for Advanced Science and Technology, The University of Tokyo, 4-6-1 Komaba, Meguro-ku, Tokyo 153-8904, Japan

Received June 6, 2000

A single crystal of the title compound $[Mn^{II}_6(H_2O)_9\{W^V(CN)_8\}_4\cdot 13H_2O]_n$ was synthesized in a hot aqueous solution containing octacyanotungstate, $Na_3[W(CN)_8]\cdot 3H_2O$, and $Mn(ClO_4)_2\cdot 6H_2O$. The compound crystallized in the monoclinic system, space group $P2_1/c$ with cell constants $a = 15.438(2)$ Å, $b = 14.691(2)$ Å, $c = 33.046(2)$ Å, $\beta = 94.832(9)°$, and $Z = 4$. The crystal consists of a $W^V-CN-Mn^{II}$ linked three-dimensional network $[\{Mn^{II}(H_2O)\}_3\{Mn^{II}(H_2O)_2\}_3\{W^V(CN)_8\}_4]_n$ and H_2O molecules as crystal solvates. There are two kinds of W sites: one is close to a dodecahedron geometry with six bridging and two terminal CN ligands; the other is close to a bicapped trigonal prism with seven bridging and one terminal CN ligands. The field-cooled magnetization measurement showed that the compound exhibits a spontaneous magnetization below $T_c = 54$ K. Further magnetization measurements on the field dependence reveal it to be a ferrimagnet where all of the Mn^{II} ions are antiparallel to all the W^V ions.

Introduction

There is a growing interest in the field of molecule-based magnets.[2−8] The properties of these materials can be modulated by a flexible molecular design. Moreover they can be synthesized at room temperature in contrast to conventional magnets. One of the important targets in this field is to obtain high-T_c molecule-based magnets.[9−12] Another is to obtain tunable magnetic materials, whose magnetic properties can be controlled by external stimuli such as light.[13−16] Hexacyanometalates $[M(CN)_6]^{n-}$ have been used recently as molecular building blocks for these purposes. As for high-T_c compounds, different formulations of a vanadium−chromium cyanide system were reported with T_c above room temperature by Verdaguer et al. ($T_c = 310$ K),[10] Miller et al. (372 K),[11] and Girolami et al. (376 K).[12] As for the triggering of magnetic properties by external stimuli, we have shown that the magnetism can be controlled by electrochemical stimuli[13] and optical stimuli[14−16] in some of the Prussian blue analogues; particularly the cobalt−iron cyanides exhibited interesting photomagnetic properties at low temperatures due to light-induced electron transfer.[14,15] In other respects, magnetic anisotropic effects were recently studied by Kahn et al. in a new family of molecule-based magnets using the low-symmetrical $[Mo^{III}(CN)_7]^{4-}$ as a building block.[17]

We are designing and preparing new types of tunable molecule-based magnetic materials. For this purpose, octacyanometalates $[M(CN)_8]^{n-}$ (M = Mo, W, ...) appear as

(1) (a) Kanagawa Academy of Science and Technology. (b) Institute of Industrial Science, the University of Tokyo. (c) Department of Materials Science and Technology, Science University of Tokyo. (d) Laboratoire de Chimie Inorganique et Matériaux Moléculaires, Université Pierre et Marie Curie. (e) Research Center for Advanced Science and Technology, the University of Tokyo.
(2) Kahn, O. *Molecular Magnetism*; VCH: New York, 1993.
(3) Miller, J. S.; Epstein, A. J. *Angew. Chem., Int. Ed. Engl.* **1994**, *33*, 385.
(4) Gatteschi, D.; et al. *Magnetic Molecular Materials*; Kluwer: Dordrecht, 1991.
(5) Tamaki, H.; Zhong, Z. J.; Matsumoto, N.; Kida, S.; Koikawa, M.; Achiwa, N.; Hashimoto, Y.; Okawa, H. *J. Am. Chem. Soc.* **1992**, *114*, 6974.
(6) Mallah, T.; Thiebaut, S.; Verdaguer, M.; Veillet, P. *Science* **1993**, *262*, 1554.
(7) William, R. E.; Girolami, G. S. *Inorg. Chem.* **1994**, *33*, 5165.
(8) Ohkoshi, S.; Abe, Y.; Fujishima, A.; Hashimoto, K. *Phys. Rev. Lett.* **1999**, *82*, 1285.
(9) Miller, J. S.; Epstein, A. J. *Science* **1991**, *252*, 1415.
(10) Ferlay, S.; Mallah, T.; Quahes, R.; Veillet, P.; Verdaguer, M. *Nature* **1995**, *378*, 701.
(11) Hatlevik, Ø; Buschmann, W. E.; Zhang, J.; Manson, J. L.; Miller, J. S. *Adv. Mater.* **1999**, *9*, 645.
(12) Holmes, S. M.; Girolami, G. S. *J. Am. Chem. Soc.* **1999**, *121*, 5593.
(13) Sato, O.; Iyoda, T.; Fujishima, A.; Hashimoto, K. *Science* **1996**, *271*, 49.
(14) (a) Sato, O.; Iyoda, T.; Fujishima, A.; Hashimoto, K. *Science* **1996**, *272*, 704. (b) Sato, O.; Einaga, Y.; Iyoda, T.; Fujishima, A.; Hashimoto, K. *J. Electrochem. Soc.* **1997**, *144*, 11. (c) Sato, O.; Einaga, Y.; Iyoda, T.; Fujishima, A.; Hashimoto, K. *Inorg. Chem.* **1999**, *38*, 4405.
(15) Bleuzen, A.; Lomench, C.; Dolbecq, A.; Villain, F.; Goujon, A.; Roubeau, O.; Nogues, M.; Varret, F.; Baudelet, F.; Dartyge, E.; Giorgetti, C.; Gallet, J.-J.; Moulin, C. C. D.; Verdaguer, M. *Mol. Cryst. Liq. Cryst.* **1999**, *335*, 253.
(16) (a) Ohkoshi, S.; Hashimoto, K. *J. Am. Chem. Soc.* **1999**, *121*, 10591. (b) Ohkoshi, S.; Hashimoto, K. *Philos. Trans. R. Soc. London A* **1999**, *357*, 2977.
(17) (a) Larionova, J.; Sanchiz, J.; Golhen, S.; Ouahab, L.; Kahn, O. *Chem. Commun.* **1998**, 953. (b) Larionova, J.; Clerac, R.; Sanchiz, J.; Kahn, O.; Golhen, S.; Ouahab, L. *J. Am. Chem. Soc.* **1998**, *120*, 13088. (c) Larionova, J.; Kahn, O.; Golhen, S.; Ouahab, L. Clerac, R. *J. Am. Chem. Soc.* **1998**, *120*, 13088.

10.1021/ic0005994 CCC: $19.00
Published on Web 10/12/2000

Table 1. Crystallographic Data for **1**

chem formula	$C_{32}H_{44}N_{32}O_{22}Mn_6W_4$	Z	4
fw	2293.93	d_{calcd} (g/cm^3)	2.041
space group	$P2_1/c$	T (K)	296(1)
a (Å)	15.438(2)	λ (Å)	0.71069
b (Å)	14.691(2)	μ (cm^{-1})	71.98
c (Å)	33.046(2)	R^a	0.046
β (deg)	94.832(9)	$R_w{}^b$	0.055
V (Å^3)	7468(1)		

^{a} $R = \sum||F_o| - |F_c||/\sum|F_o|$. ^{b} $R_w = [\sum w(|F_o| - |F_c|)^2/\sum wF_o^2]^{1/2}$.

Table 2. Selected Bond Angles (deg)

Mn(1)	N(11)	C(11)	162.6(9)	Mn(2)	N(12)	C(12)	166(1)
Mn(2)	N(12a)	C(12a)	173.8(10)	Mn(3)	N(13a)	C(13a)	176.9(9)
Mn(5)	N(15)	C(15)	165.6(9)	Mn(6)	N(16)	C(16)	178(1)
Mn(1)	N(21)	C(21)	169.7(10)	Mn(1)	N(21a)	C(21a)	154.5(10)
Mn(2)	N(22b)	C(22b)	154.5(8)	Mn(3)	N(23)	C(23)	167.6(9)
Mn(3)	N(23a)	C(23a)	164.5(10)	Mn(4)	N(24)	C(24)	162.8(9)
Mn(5)	N(25a)	C(25a)	164(1)	Mn(1)	N(31)	C(31)	165.9(9)
Mn(3)	N(33a)	C(33a)	163.1(9)	Mn(4)	N(34)	C(34)	169(1)
Mn(4)	N(34c)	C(34c)	169(1)	Mn(5)	N(35)	C(35)	165.5(9)
Mn(6)	N(36)	C(36)	176.9(9)	Mn(6)	N(36c)	C(36c)	159.6(10)
Mn(1)	N(41)	C(41)	161.4(9)	Mn(2)	N(42)	C(42)	165.9(9)
Mn(2)	N(42a)	C(42a)	176.2(9)	Mn(3)	N(43)	C(43)	165.0(10)
Mn(4)	N(44)	C(44)	173.6(9)	Mn(5)	N(45b)	C(45b)	164(1)
Mn(6)	N(46)	C(46)	164.7(10)	W(1)	C(10i)	N(10i)	179(1)
W(1)	C(10j)	N(10j)	178(1)	W(1)	C(11)	N(11)	177.8(9)
W(1)	C(12)	N(12)	175(1)	W(1)	C(12a)	N(12a)	177.8(9)
W(1)	C(13a)	N(13a)	176.3(9)	W(1)	C(15)	N(15)	178.2(9)
W(1)	C(16)	N(16)	177.7(10)	W(2)	C(20)	N(20)	174(1)
W(2)	C(21)	N(21)	178.4(10)	W(2)	C(21a)	N(21a)	176.9(9)
W(2)	C(22b)	N(22b)	177.4(9)	W(2)	C(23)	N(23)	177.3(10)
W(2)	C(23a)	N(23a)	178.9(9)	W(2)	C(24)	N(24)	173.2(9)
W(2)	C(25a)	N(25a)	175.5(10)	W(3)	C(30)	N(30)	178(1)
W(3)	C(31)	N(31)	176.7(10)	W(3)	C(33a)	N(33a)	176.8(10)
W(3)	C(34)	N(34)	176.3(10)	W(3)	C(34c)	N(34c)	179(1)
W(3)	C(35)	N(35)	174.9(10)	W(3)	C(36)	N(36)	178.5(9)
W(3)	C(36c)	N(36c)	178.7(10)	W(4)	C(40)	N(40)	179(1)
W(4)	C(41)	N(41)	177.3(9)	W(4)	C(42)	N(42)	178.9(9)
W(4)	C(42a)	N(42a)	176.3(10)	W(4)	C(43)	N(43)	175.6(9)
W(4)	C(44)	N(44)	174.3(9)	W(4)	C(45b)	N(45b)	178.5(9)
W(4)	C(46)	N(46)	174.4(10)				

versatile building blocks. These species might show various geometrical structures (e.g., square antiprism, dodecahedron, bicapped trigonal prism) depending on the external environments.[18] This flexibility may be advantageous in bringing out the tunable property. Furthermore, an enhanced exchange interaction may be expected due to the increased overlap between the diffuse orbitals of 4d or 5d metal ions and those of 3d metal ions. We have obtained a new family of molecule-based magnets $A_xM'_y[M(CN)_8]$ (A = alkali metal ions) derived from $[M(CN)_8]^{3-}$ (M = Mo, W) units and simple metal ions (M′ = Mn, Co, Ni, Cu)[19,20] and observed photomagnetic effects in some of these compounds.[19] Although structural information is obviously important in understanding the magnetic properties and photomagnetic properties of these compounds, to our knowledge no crystal structures of three-dimensional metal assemblies derived from $[M(CN)_8]^{n-}$ and simple metal ions have been reported so far. This paper provides for the first time the result of the single-crystal X-ray crystallography of one of the compounds in this family, $[Mn_6(H_2O)_9\{W(CN)_8\}_4\cdot 13\ H_2O]_n$. The magnetic properties of this compound are also described.

Experimental Section

Preparations. $Na_3[W(CN)_8]\cdot 3H_2O$ was prepared according to the literature method.[21] The aqueous solutions of $Na_3[W(CN)_8]\cdot 3H_2O$ and $Mn(ClO_4)_2\cdot 6H_2O$ were mixed and then allowed to stand for about a week at 50 °C in a brown bottle. Red and yellow single crystals were obtained. The red one is the title compound, $[Mn^{II}_6(H_2O)_9\{W^V(CN)_8\}_4\cdot 13H_2O]_n$ **(1)**, while the yellow one is of the composition $[\{Mn^{II}(H_2O)_2\}_2\{W^{IV}(CN)_8\}\cdot 4H_2O]_n$. The structure and properties of the latter will be described elsewhere. Polymeric W^V-Mn^{II} compounds can also be prepared at room temperature under similar conditions, which were obtained only as the microcrystals with a slightly different composition.

Crystallographic Data Collection and Structure Determination. The red plate crystal having approximate dimensions of 0.40 × 0.30 × 0.10 mm was mounted in a glass capillary. All measurements were made on a Rigaku AFC7R diffractometer with graphite-monochromated Mo Kα radiation and a rotating anode generator. The data were collected at a temperature of 23 ± 1 °C using the ω-scan technique to a maximum value of $2\theta = 55.1°$ at a scan speed of 16. 0°/min (in ω). Of the 17777 reflections which were collected, 17142 were unique ($R_{int} = 0.070$), 12478 reflections observed [$I > 3.00\sigma(I)$]. The intensities of three representative reflections were measured after every 150 reflections, which revealed no significant decay during the data correction. The data were corrected for Lorentz and polarization effects and for absorption, from which 12478 reflections [$I > 3.00\sigma(I)$] were used in the following calculations. The structure was solved by the direct method and expanded using Fourier techniques. The non-hydrogen atoms were refined anisotropically, whereas the hydrogen atoms of the water molecules were not included in the refinements. All calculations were performed using the teXsan crystallographic software package of Molecular Structure Corporation.[22] The crystallographic data are given in Table 1.

Physical Measurements. The infrared spectrum was measured with a Shimadzu FT-IR 8200PC spectrometer. Magnetization measurements were carried out with a Quantum Design MPMS-5S superconducting quantum interference device (SQUID) magnetometer working down to 1.9 K and up to 50 kG.

Results and Discussion

IR Spectrum. The title compound shows two $\nu_{(C\equiv N)}$ band modes at 2196 and 2172 cm^{-1} with two shoulders around 2160 and 2140 cm^{-1} in its IR spectrum. The band at 2140 cm^{-1} is analogous to the $\nu_{(C\equiv N)}$ band of $(HBu_3N)_3[W(CN)_8]$ (HBu_3N

Table 3. Selected Torsion Angles (deg)

W(1)	C(11)	N(11)	Mn(1)	24(26)
W(1)	C(12)	N(12)	Mn(2)	56(15)
W(1)	C(12a)	N(12a)	Mn(2)	105(25)
W(1)	C(13a)	N(13a)	Mn(3)	64(27)
W(1)	C(15)	N(15)	Mn(5)	1(34)
W(1)	C(16)	N(16)	Mn(6)	−104(36)
W(2)	C(21)	N(21)	Mn(1)	−29(37)
W(2)	C(21a)	N(21a)	Mn(1)	61(18)
W(2)	C(22b)	N(22b)	Mn(2)	−25(20)
W(2)	C(23)	N(23)	Mn(3)	105(19)
W(2)	C(23a)	N(23a)	Mn(3)	−79(53)
W(2)	C(24)	N(24)	Mn(4)	−70(8)
W(2)	C(25a)	N(25a)	Mn(5)	49(16)
W(3)	C(31)	N(31)	Mn(1)	−8(18)
W(3)	C(33a)	N(33a)	Mn(3)	−83(17)
W(3)	C(34)	N(34)	Mn(4)	−81(17)
W(3)	C(34c)	N(34c)	Mn(4)	−26.4
W(3)	C(35)	N(35)	Mn(5)	−1(13)
W(3)	C(36)	N(36)	Mn(6)	148(24)
W(3)	C(36c)	N(36c)	Mn(6)	−143(42)
W(4)	C(41)	N(41)	Mn(1)	43(21)
W(4)	C(42)	N(42)	Mn(2)	−18(52)
W(4)	C(42a)	N(42a)	Mn(2)	43(27)
W(4)	C(43)	N(43)	Mn(3)	−111(11)
W(4)	C(44)	N(44)	Mn(4)	−20(16)
W(4)	C(45b)	N(45b)	Mn(5)	135(38)
W(4)	C(46)	N(46)	Mn(6)	40(12)

(18) Leipoldt, J. G.; Basson, S. S.; Roodt, A. *Adv. Inorg. Chem.* **1993**, *32*, 241.
(19) Hashimoto et al. Work in progress.
(20) Verdaguer, M.; Desplanches, C.; Sieklocka, B. Work in progress.
(21) Pribush, R. A.; Archer, R. D. *Inorg. Chem.* **1974**, *13*, 2556.
(22) teXsan: *Crystal Structure Analysis Package*, Molecular Structure Corporation (1985, 1992).

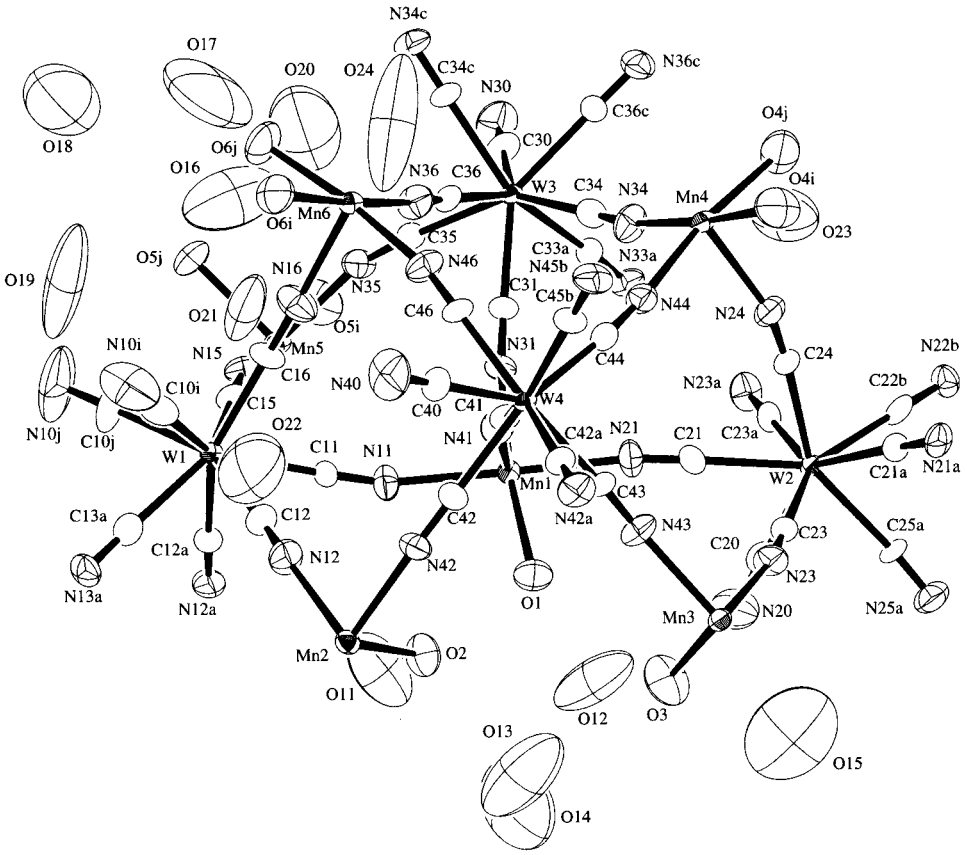

Figure 1. Structure of the $\{Mn^{II}(H_2O)\}_3\{Mn^{II}(H_2O)_2\}_3\{W^V(CN)_8\}_4 \cdot 13H_2O$ asymmetrical unit. Ellipsoids at the 50% probability level.

= tributylammonium) and can be attributed to a terminal cyanide group. It is well-known that a shift of $\nu_{(C\equiv N)}$ to high frequency is observed in most cases of the hexacyanometalate-based compounds due to the N coordination to other metal ions.[10,11] A similar trend was also reported on a series of octacyanomolybdate(IV)−M(II) polymers.[23] Therefore, the remaining three bands at higher frequency are attributed to the bridging cyanide groups. The higher frequency bands are stronger than the lower one, suggesting that most of the CN groups are bridging. This is in accord with the X-ray structure.

Crystal Structure. The crystal consists of a three-dimensional network $[\{Mn^{II}(H_2O)\}_3\{Mn^{II}(H_2O)_2\}_3\{W^V(CN)_8\}_4]_n$ and H_2O molecules as crystal solvates. The structure of the asymmetric unit $\{Mn^{II}(H_2O)\}_3\{Mn^{II}(H_2O)_2\}_3\{W^V(CN)_8\}_4 \cdot 13H_2O$ is shown in Figure 1. The W sites can be classified into two groups; one is W1, and the other is (W2, W3, W4). The geometry around W1 is close to a dodecahedron, where six CN ligands are bridged with Mn and the other two are terminal ones. W2, W3, and W4 atoms are each surrounded by seven −CN−Mn linkages and one terminal CN ligand. Their geometry is close to a bicapped trigonal prism. As for Mn sites, there are also two different sites, MnA (A = 1, 2, 3) and MnB (B = 4, 5, 6). MnA sites are surrounded by five −NC−W linkages and one water molecule. MnB sites are surrounded by four −NC−W linkages and two water molecules in cis conformation. The geometry around the Mn ions is described as a distorted octahedron.

The Mn−N bond lengths range from 2.173(9) to 2.257(9) Å, and the Mn−O from 2.163(9) to 2.271(8) Å. The bond angles range from 81.7(4)° to 103.4(4)° and from 162.5(4)° to 179.1(4)°, respectively instead of 90° and 180° for an ideal octahedron. The bond angles and torsion angles around the Mn−N−C−W linkages are listed in Tables 2 and 3, respectively. Although all the W−C−N bond angles are close to 180° (173−179°), the Mn−N−C bond angles significantly deviate from 180°, ranging from 154.5(8)° to 178.1° (the mean value is 166.7°). The torsion angles of Mn−N−C−W show various values. In most cases, the absolute values of the torsion angles are larger than 10°. These data clearly show that most of the Mn−N−C−W linkages are considerably far from being linear and coplanar.

The environment near the asymmetric unit is shown in Figure 2. The five W atoms form a tetragonal pyramid. The W1, W4, W2, and W2* atoms build the basal plane, and W3 lies at the apex at a distance of 5.50 Å from the basal plane. The Mn1 atom is at the center of a square plane with a small shift (<0.3 Å) from the basal W1−W4−W2−W2* plane. Each face of the W square pyramid is capped by a Mn atom (Mn4, Mn5, Mn6, or Mn3*) through three W−CN−Mn linkages. In addition, the W atoms on the three edges of the basal plane, W4−W1, W2−W4, and W1−W2*, are bridged by the Mn2, Mn3, and Mn2*′ atoms, respectively, while the W atoms on the other bridge (W2−W2*) are not bridged by the corresponding Mn4* atom (Mn4*−N20 = 4.08(1) Å). The structure of the W_5Mn_9 unit in Figure 2 is similar to that of the M_6Mn_9 (M = W, Mo) spin cluster previously reported,[24] but here one W atom is substituted by a H_2O molecule.

Let us see how the network structure forms. First, the W_5 motifs share W2 to form a chain along the 2-fold screw axis with a dihedral angle of 10° between the two basal planes of

(23) Mcknight, G. F.; Haight, G. P., Jr. *Inorg. Chem.* **1973**, *12*, 3007.

(24) (a) Zhong, Z. J.; Seino, H.; Mizobe, Y.; Hidai, M.; Fujishima, A.; Ohkoshi, S.; Hashimoto, K. *J. Am. Chem. Soc*. **2000**, *122*, 2952. (b) Larionova, J.; Gross, M.; Pilkington, M.; Andres, H.; Stoeckli-Evans, H.; Güdel, H. U.; Decurtins, S. *Angew. Chem., Int. Ed.* **2000**, *39*, 1605.

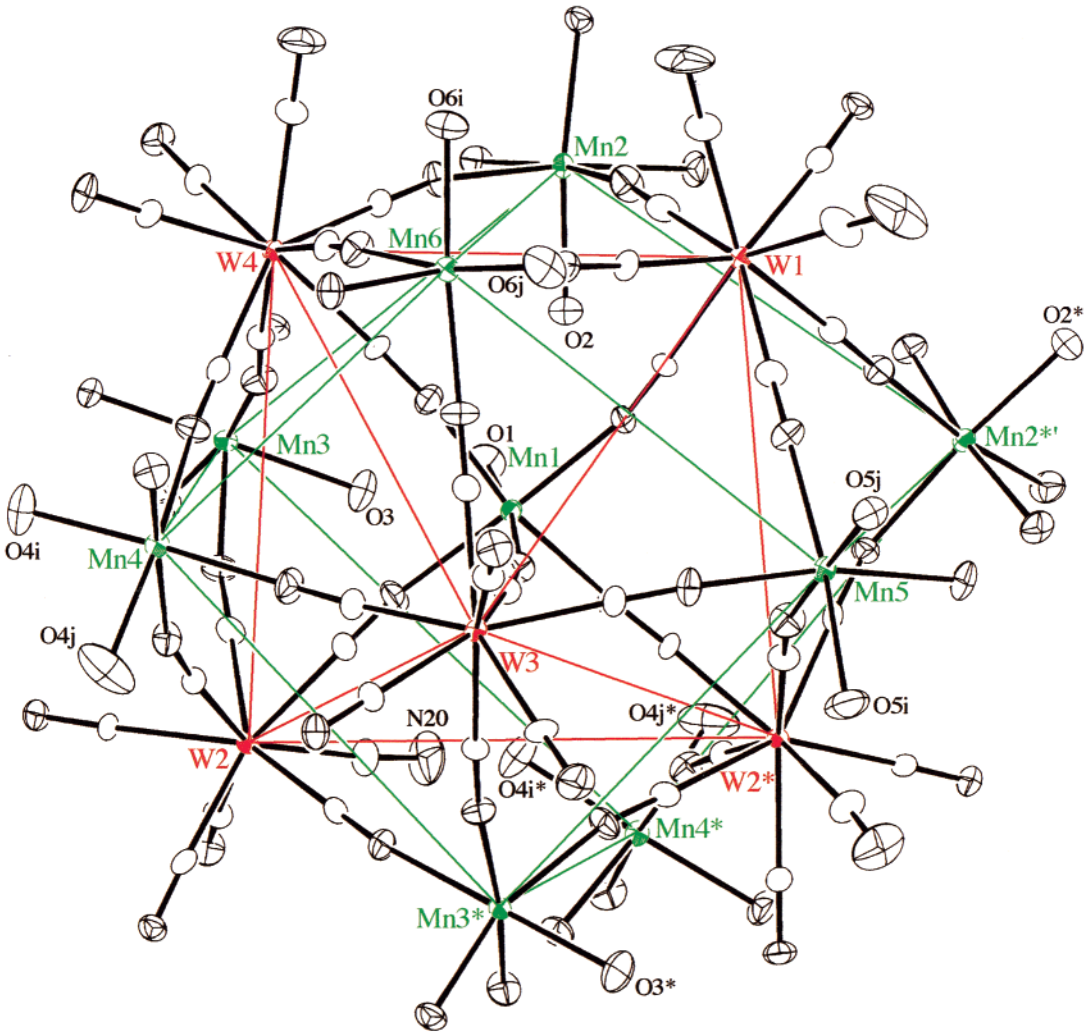

Figure 2. Structure of the W_5Mn_9 unit (red line, W_5 square pyramid; green lines, Mn_8 hexahedron). Ellipsoids at the 30% probability level.

the adjacent motifs (Figure 3). In this chain, Mn3 is shared by two motifs, capping the W2−W3^{v}−W2^{v} face of one motif and bridging the W2−W4 edge of another. The Mn2*′ bridging the edge W1−W2* and the Mn5 capping the W1−W3−W2* face are linked to W4^ of the next adjacent W_5 unit in the same chain through a NC bridge (Figure 3, cyan line). Each chain is linked to other two chains along the *a*-axis and *c*-axis (Figure 4). Appearing by an operation of inversion, the distance between the chains along the *c*-axis is shorter than that along the *a*-axis. The interchain W3−W3″ distance along the *c*-axis is 6.550(1) Å. The two W_5 units related to an inversion center are connected between the face-capping Mn4, Mn6 (Mn4″, Mn6″) and the opposite W3″ (W3) through four linkages (W3−CN−Mn4″, W3−CN−Mn6″, W3′−CN−Mn4, W3′−CN−Mn6). Conversely, the interchain W1−W4* distance of 7.561(1) Å is observed between the chains obtained by an operation of translation along the *a*-axis. Along this direction, the Mn2*′ is shared by two motifs by bridging the W1−W2* and W1*′−W4*′ edges. The edge-bridging Mn3^ (or Mn3^′) is linked to the opposite W1*′ (or W1) through a NC bridge. In this way, the W_5 motifs form a chain by W−CN−Mn linkages with a common apex of the basal plane, and then the four neighboring chains are linked through Mn atoms to form a three-dimensional structure.

Noncoordinated water molecules are located in the voids of the three-dimensional network. As listed in Table 4, hydrogen bonds exist not only between noncoordinated water molecules

Table 4. Hydrogen Bonds (Å) [O(*m*): $m \ll 6$, Coordinated H_2O; $m > 6$, Noncoordinated H_2O. N: Nonbridging Cyano N]

O(1)	O(12)	2.66(2)	O(1)	O(11)	3.49(2)
O(2)	O(11)	2.72(2)	O(2)	O(13)	2.83(2)
O(3)	O(18)	2.85(3)	O(3)	O(15)	2.94(3)
O(3)	O(12)	2.96(2)	O(3)	O(13)	3.13(3)
O(4i)	O(17)	2.77(2)	O(4i)	O(5i)	3.13(1)
O(4i)	O(12)	3.14(2)	O(4i)	O(15)	3.19(3)
O(4j)	O(14)	2.82(2)	O(4j)	O(23)	3.07(2)
O(5i)	O(20)	2.55(4)	O(5i)	O(15)	2.95(3)
O(5i)	O(20)	3.34(5)	O(5j)	O(19)	2.69(2)
O(5j)	O(17)	3.23(3)	O(5j)	O(20)	3.28(4)
O(5j)	O(16)	3.38(2)	O(6i)	O(21)	2.81(2)
O(6i)	O(6i)	3.41(2)	O(6i)	O(21)	3.43(2)
O(6i)	O(24)	3.43(4)	O(6j)	O(16)	2.87(2)
O(6j)	O(21)	2.76(1)	O(11)	O(14)	3.59(3)
O(12)	O(14)	2.70(3)	O(12)	O(13)	3.49(3)
O(13)	O(18)	3.14(4)	O(13)	O(14)	3.35(3)
O(14)	O(22)	2.86(4)	O(15)	O(17)	3.05(4)
O(15)	O(18)	3.22(3)	O(15)	O(20)	3.31(5)
O(16)	O(17)	2.79(3)	O(17)	O(20)	2.80(5)
O(17)	O(18)	2.87(3)	O(18)	O(19)	3.57(3)
O(18)	O(24)	3.52(7)	O(19)	O(19)	3.26(3)
O(19)	O(24)	3.35(4)	O(21)	O(22)	2.92(3)
O(22)	O(23)	2.75(3)			
O(6i)	N(10i)	2.85(2)	O(23)	N(10i)	3.02(2)
O(24)	N(10i)	3.37(4)	O(13)	N(10j)	3.52(3)
O(18)	N(10j)	3.03(3)	O(19)	N(10j)	3.10(2)
O(19)	N(10j)	3.14(2)	O(24)	N(10j)	3.14(4)
O(12)	N(20)	3.21(2)	O(15)	N(20)	3.49(3)
O(5i)	N(30)	3.59(2)	O(5j)	N(30)	2.86(1)
O(15)	N(30)	3.56(3)	O(18)	N(30)	3.39(4)
O(24)	N(30)	3.35(5)	O(20)	N(30)	3.00(5)
O(20)	N(30)	3.48(4)	O(14)	N(40)	3.29(2)
O(21)	N(40)	3.12(2)	O(22)	N(40)	3.23(3)

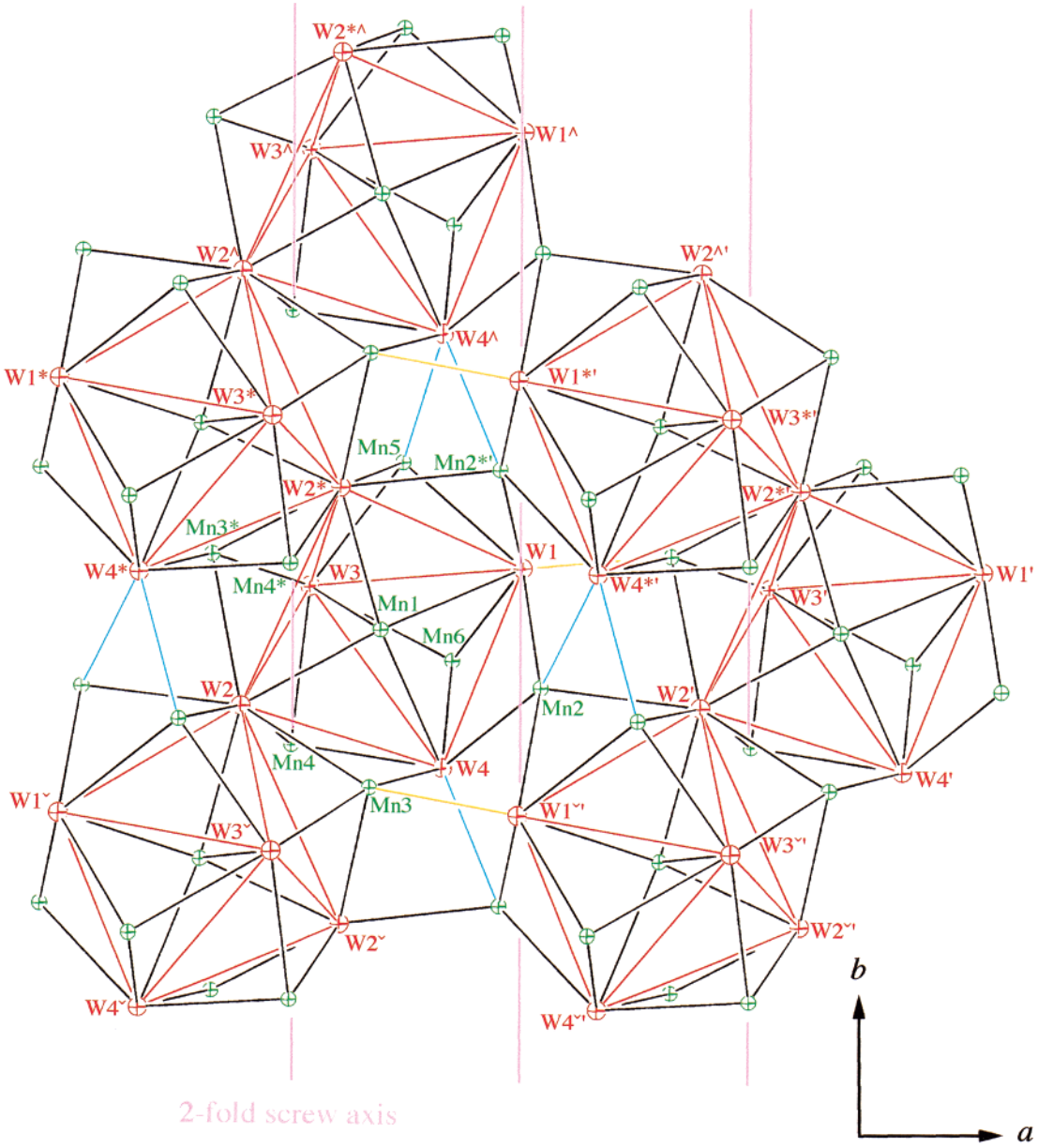

Figure 3. Structure of **1** in the *ab*-plane (red line, W_5 square pyramid; black lines, W−CN−Mn bridges within W_5 motif; cyan lines, special W−CN−Mn bridges within one-dimensional chain; orange lines, special W−CN−Mn bridges between chains; pink lines, 2-fold screw axes).

but also between noncoordinated and coordinated water molecules. It is notable that all the nonbridging CN groups are also hydrogen-bonded with either noncoordinated or coordinated water molecules.

Magnetic Properties. The product of the molar magnetic susceptibility and the temperature, $\chi_M T$, as a function of T is shown in Figure 5. At room temperature $\chi_M T$ is 24.7 (cm^3 K mol^{-1}), smaller than the value (27.75) of the six isolated Mn^{II} ($S = {}^5/_2$) ions and four isolated W^V ($S = {}^1/_2$) ions, suggesting appreciable antiferromagnetic interaction present. On cooling, $\chi_M T$ monotonically increased first very slowly and then rapidly below 80 K up to a maximum value around 50 K. The maximum $\chi_M T$ value depends on the applied field. The low-temperature data suggest that the compound exhibits a long-range magnetic ordering. This is confirmed by the field-cooled-magnetization (FCM) curve in Figure 6. The FCM curve obtained in cooling the sample with an applied field of 10 G displays a sharp increase around 54 K and a rapid tendency toward saturation, clearly demonstrating a long range order transition. The field dependence of the magnetization at 5 K is given in Figure 7. The magnetization increases very rapidly at low field, as expected for a magnet, and then increases much more slowly above 2 kG. The magnetization under 50 kG is found equal to 25.40 $N_A\beta$. This value is close to the expected saturation value (26.0 $N_A\beta$) when the six spins ${}^5/_2$ of the Mn^{II} ions of the molecular unit are antiparallel to the four spins ${}^1/_2$ of the W^V ions. This magnetization behavior clearly reveals that a short-range antiferromagnetic interaction operates between the Mn^{II} and W^V ions and the compound is a ferrimagnet. The absence of a minimum in the $\chi_M T$ versus T curve, the signature of ferrimagnetism, is only contradictory in appearance. The minimum can be located above the temperature range explored. No hysteresis is observed, demonstrating a weak anisotropy, one of the reasons being the small anisotropy of the Mn^{II} ion.

It is not easy to rationalize the antiferromagnetic short-range interaction in the present system. There are different W and Mn surroundings, each in low symmetry, and there are many different W−CN−Mn bridging schemes with different W−C−N and C−N−Mn angles and different W−C−N−Mn torsion angles. Therefore, the symmetry of the $(NC)_7W-CN-Mn(NC)_n$-

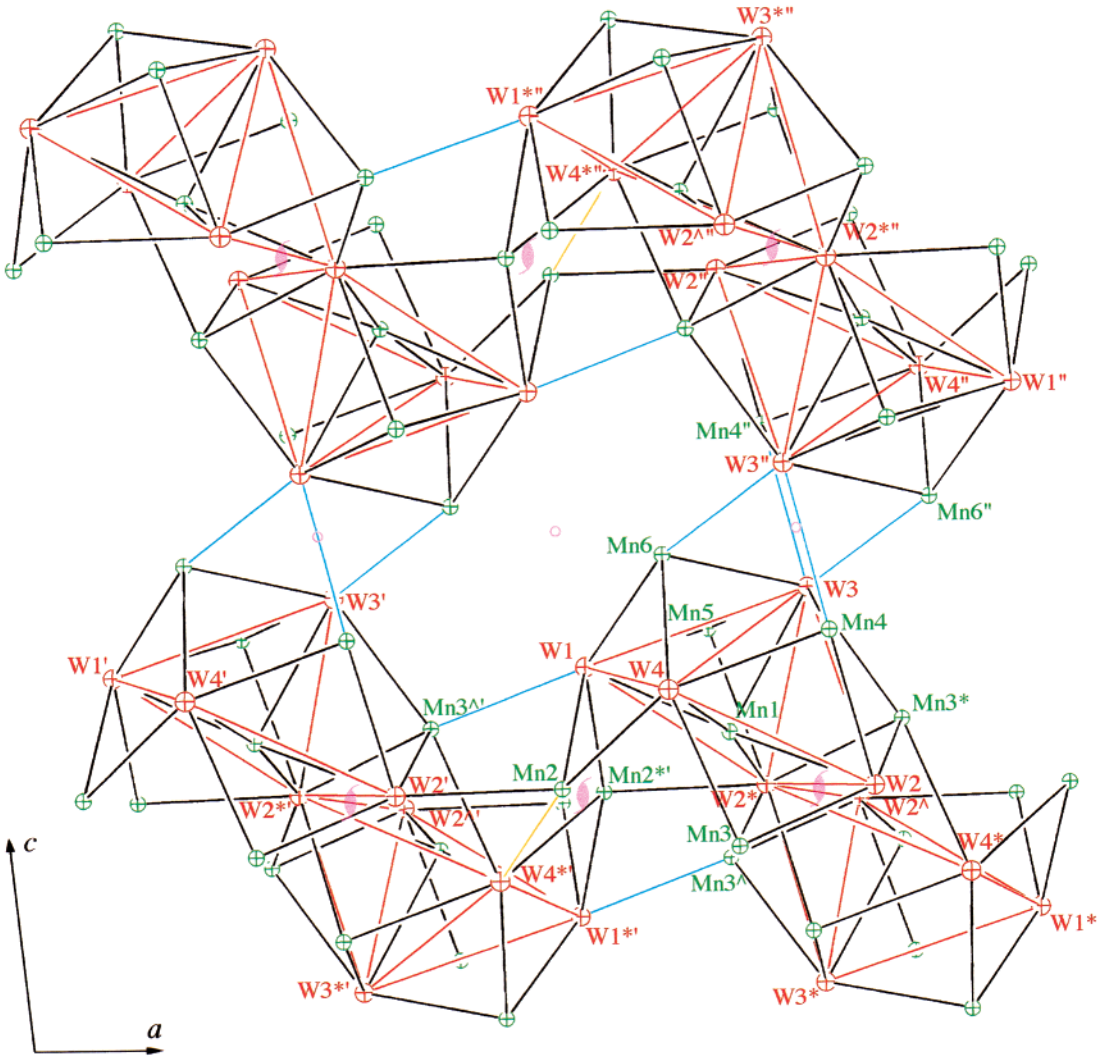

Figure 4. Structure of **1** in the *ac*-plane (red and black lines, same as in Figure 3; orange lines, special W−CN−Mn bridges within one-dimensional chain; cyan lines, special W−CN−Mn bridges between chains; ○, inversion centers; symbol that resembles a $\oint$, 2-fold screw axes).

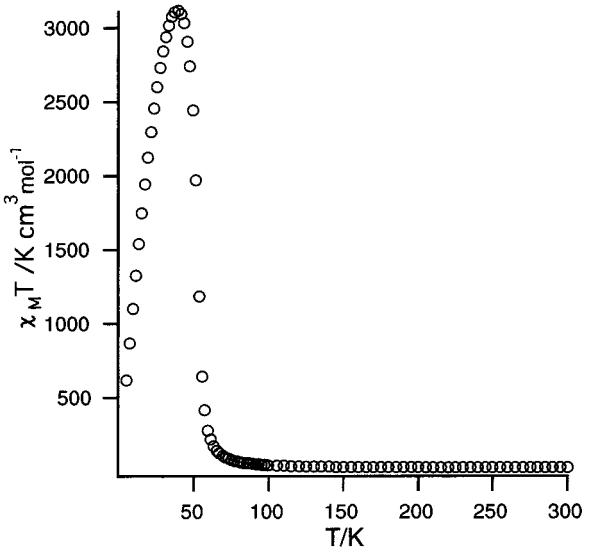

Figure 5. $\chi_M T$ versus T curve for **1** at an external field of 1000 G.

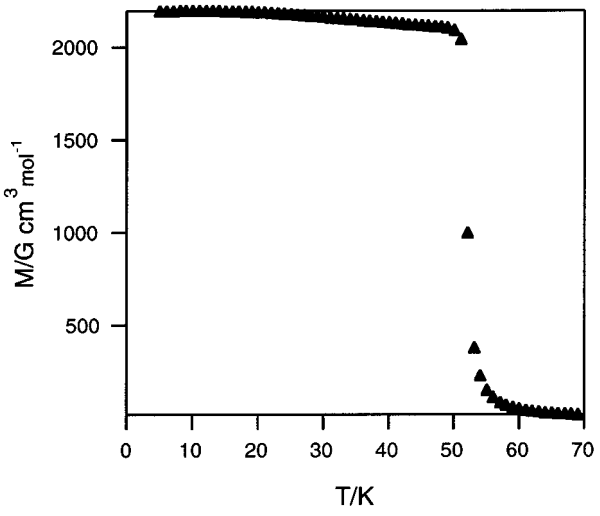

Figure 6. FCM curve of **1** under 10 G.

$(OH_2)_{6-n}$ bridge is very low and the overlap of the unique W magnetic orbital with the five Mn ones is the most likely situation which favors antiferromagnetic coupling. The predominant one may be the $\pi-\pi$ interaction through the π system of the cyanide (Scheme 1a), reminiscent of the case of a linear arrangement as in the Prussian blue families ($xz-xz$ interaction, Scheme 1b). In the two cases, the schemes represent only the bonding combination of nonbonded magnetic orbitals. This is in contrast with the case of the heptacyano $Mo^{III}-Mn^{II}$ compound reported by Kahn et al., where a ferromagnetic interaction was reported.[17]

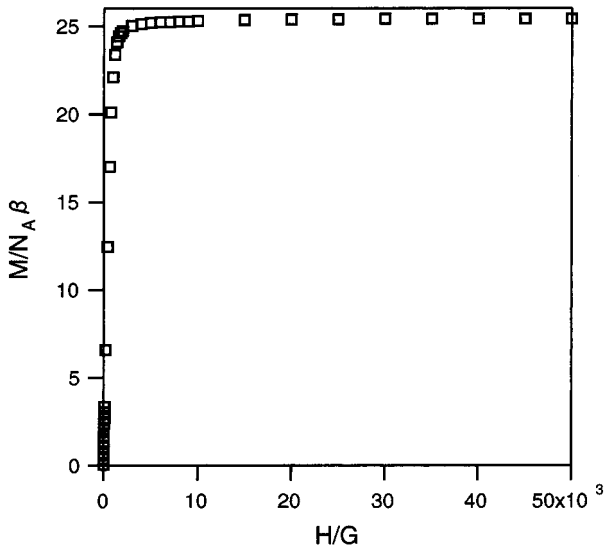

Figure 7. Field dependence of the magnetization for **1** at 5 K.

In conclusion, by modulating the reaction conditions we succeeded in obtaining a $W^V_4-Mn^{II}_6$ polymeric compound as a single crystal and we revealed the complicated three-dimensional network by X-ray analysis, which is the first example in a series of bimetallic assemblies from paramagnetic octacyanometalates.[25] Two interesting features may be underlined: (a) the different geometries of W and Mn sites present in the same structure suggest that the flexibility of the octacyanometalates and their coordination ability remain important, even in three-dimensional structures; (b) the Curie temperature $T_c = 54$ K is much higher than that of the Prussian blue analogue $Mn^{II}_{1.5}[Fe^{III}(CN)_6]\cdot 12H_2O$ ($T_c = 9$ K) with similar spin carriers ($S_{Mn} = {}^5/_2$, $S_{Fe} = {}^1/_2$). The increase of T_c is partially due to the larger number of magnetic neighbors but can be mostly attributed to an enhanced magnetic exchange interaction due to the larger diffusing 5d orbitals of W. These two features make octacyanometalates good molecular precursors for new magnetic systems of various dimensionalities.

(25) Other studies will be reported soon by our groups and the group of S. Decurtins.

Scheme 1

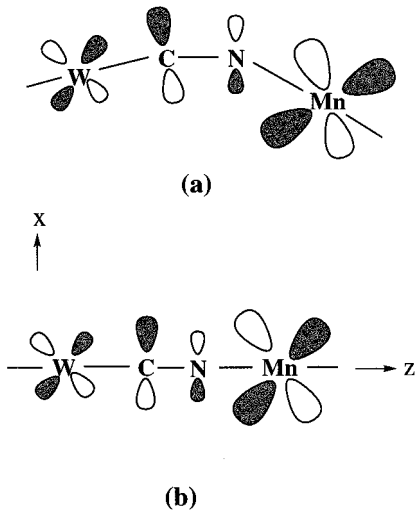

Acknowledgment. This work was partially supported by a Grant-in-Aid for Scientific Research on Priority Areas (Metal-assembled Complexes). We thank C. Desplanches for many fruitful discussions.

Supporting Information Available: An X-ray crystallographic file in CIF format for the structure of **1**. This material is available free of charge via the Internet at http://pubs.acs.org.

IC0005994